



ORIGINAL ARTICLE

The erbB2+ cluster of the intrinsic gene set predicts tumor response of breast cancer patients receiving neoadjuvant chemotherapy with docetaxel, doxorubicin and cyclophosphamide within the GEPARTRIO trial

A. Rody^{a,*}, T. Karn^a, C. Solbach^a, R. Gaetje^a, M. Munnes^b, S. Kissler^a, E. Ruckhäberle^a, G.v. Minckwitz^a, S. Loibl^a, U. Holtrich^a, M. Kaufmann^a

^aDepartment of Obstetrics and Gynecology, J. W. Goethe-University, Theodor-Stern-Kai 7, 60590 Frankfurt, Germany

^bBayer Healthcare AG, Leverkusen, Germany

Received 12 December 2006; received in revised form 21 February 2007; accepted 26 February 2007

KEYWORDS

Intrinsic gene set;
Molecular classification;
ErbB2;
Neoadjuvant chemotherapy;
Breast cancer

Summary Gene expression profiling using Affymetrix HG-U133 Arrays (22,500 genes) was performed on fresh frozen pretherapeutic core biopsies from 50 patients undergoing neoadjuvant chemotherapy (NAC) with docetaxel, adriamycin, cyclophosphamide (TAC) within the GEPARTRIO trial.

The Sorlie classification based on the “intrinsic gene set” revealed four different subgroups in our cohort (normal-like: 14%, basal-like: 20%, erbB2+: 22% and luminal: 44%), which is in line with the original description. High genomic grade but not histopathological grading was statistically different within the four subgroups ($P < 0.001$). About 45.5% of tumors classified according to erbB2+ cluster showed a pathological complete response compared to 0% in the normal-like, 10.0% in the basal-like and 9.1% in the luminal subgroup ($P = 0.024$). There was a trend to less tumor relapses in the erbB2+ subgroup (0%) compared to the normal-like (28.6%), basal-like (30.0%) and luminal (13.6%) cluster ($P = 0.215$).

Our data suggest that the molecular tumor subtypes based on the “intrinsic gene set” can be used to predict tumor response according to NAC.

© 2007 Elsevier Ltd. All rights reserved.

*Corresponding author. Tel.: +49 69 6301 4117; fax: +49 69 6301 83469.
E-mail address: achim.rody@em.uni-frankfurt.de (A. Rody).

Introduction

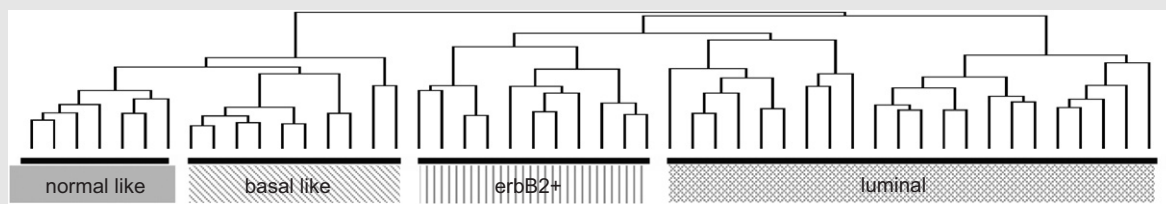
Neoadjuvant chemotherapy (NAC) is a valid option not only for advanced breast cancer stages but even for operable breast cancer. Response to NAC is a predictor of long-term outcome and gives immediate prognostic information in contrast to adjuvant trials where results are revealed only after long term follow-up. However, it is essential in this setting to define subgroups of patients, which strongly benefit from NAC and have a high probability to respond with a pathological complete response (pCR). While it was shown that estrogen receptor negative tumors demonstrate more often a pCR¹ there is nevertheless a sufficient number of patients with estrogen receptor positive breast cancer who experience a pCR after NAC. Thus, new classifiers are needed helping to define those tumor subgroups with a high chance of achieving a pCR, even when classical prognostic or predictive markers do not indicate this. Global gene expression profiling by microarrays has been used as a valuable tool for the identification of prognostic marker genes.^{2–5} Perou et al. reported that gene expression profiling by DNA microarray analysis of breast tumors is feasible and allows to distinguish different tumor subtypes.⁶ A further important step was the molecular classification of breast carcinomas based on gene expression patterns in luminal A and B, basal-like, erbB2+ and normal breast-like subtypes and their correlation with overall and disease-free survival by Sorlie et al.² As demonstrated by several groups this classification showed a high reproducibility⁷ and thus should be appropriate for further investigations. Recently, Rouzier et al. could demonstrate that basal-like and erbB2+ subtypes of breast cancer are more sensitive to neoadjuvant paclitaxel- and doxorubicin-containing chemotherapy.⁸ Goal of our study was to investigate if this observation can be verified in patients receiving neoadjuvant combination chemotherapy consisting of docetaxel (T), doxorubicin (A) and cyclophosphamide (C) within the GEPAR-TRIO trial.

Material and methods

Pretherapeutic core biopsies were obtained from 70 patients. Samples were snap frozen in liquid nitrogen and part of the removed tumor tissue was used for diagnostic purposes. One 5 μ m tissue section (usually after 15 30- μ m sections) of each biopsy and the first and the last section of each remaining tumor were stained with hematoxylin and eosin to monitor the tumor cell percentage of

the tissue. Only specimens with $\geq 80\%$ of tumor cells were included in further analysis. RNA was isolated with Qiagen RNeasy reagents and expression profiling performed using Affymetrix Hg U133 Arrays (22,500 genes). More than two-thirds of the biopsies yielded sufficient amounts ($> 5 \mu$ g) of RNA for expression profiling and high-quality chip data were obtained for 50 samples. Clinical characteristics of these 50 patients (median age 53, range 30–69) have already been described⁹ and are iterated in Table 1. Quality control analysis of extracted total RNA was performed with Agilent Bioanalyzer 2100 (capillary gel electrophoresis) and photometric quantification of the isolated total RNA was determined by NanoDrop ND-1000. Samples were characterized according to standard pathology including IHC of ER, PR and HER2 and amount of cancer cells as well as FISH analysis of HER2.

Expression profiling was performed using Affymetrix Hg U133 Arrays (22,500 genes) as described elsewhere.^{10,11} Hybridization intensity data were automatically acquired and processed by Affymetrix Microarray Suite 5.0 software. Subsequently, data were analyzed by the EXPRESSIONIST software from GeneData (Basel, Switzerland) using the PM-MM model to obtain raw expression levels. The expression level of each gene was determined by calculating the average of differences in intensity (perfect match–mismatch) between its probe pairs. Scans were rejected if the scaling factor exceeded 2 or “chip surface scan” revealed scratches, specks or gradients affecting overall data quality (Refiner, GeneData AG, Basle, Switzerland). The data were then further analyzed by using the Cluster and Treeview software package¹² and SPSS (SPSS Inc., Chicago, IL). Prior to cluster analysis gene chip expression values were adjusted by log transformation and median centering of the arrays. For sample classification, we performed an unsupervised hierarchical clustering using 120 Affymetrix Probe Sets which characterize the four different intrinsic molecular tumor classes. These 120 Affymetrix probe sets correspond to the described intrinsic gene set markers and were identified by mapping the probe sequences of Sorlie et al.² via Unigene clusters to Affymetrix sequences. The list of these 120 probe sets is presented in Supplementary Table ST1. Hierarchical clustering was performed using the Pearson correlation as similarity metric and complete linkage. Similar results were obtained when 298 probe sets proposed by Rouzier et al.⁸ were used for stratification. The “genomic grading” was assessed by hierarchical clustering based on 242 probe sets as described by Sotiriou et al.¹³

Table 1 Correlation of molecular subtype and clinico-pathological data.

n (%)	Total	Molecular subtype				P-value
		Normal-like 7 (14.0%)	Basal-like 10 (20.0%)	erbB2+ 11 (22.0%)	Luminal 22 (44.0%)	
<i>Menopausal status</i>						
Premenopausal	25	4 (57.1%)	6 (60.0%)	7 (63.6%)	8 (36.4%)	0.392
<i>Tumor size</i>						
T2	34	3 (42.9%)	7 (70.0%)	9 (81.8%)	15 (68.2%)	0.135
T3	10	1 (14.3%)	3 (30.0%)	2 (18.2%)	4 (18.2%)	
T4	63	4 (42.9%)	0 (0.0%)	0 (0.0%)	3 (13.6%)	
<i>Tumor stage</i>						
Stage II A	22	2 (28.6%)	4 (40.0%)	6 (54.5%)	10 (45.5%)	0.275
Stage II B	16	2 (28.6%)	4 (40.0%)	3 (27.3%)	7 (31.8%)	
Stage III A	6	0 (0%)	2 (20.0%)	2 (18.2%)	2 (9.1%)	
Stage III B	6	3 (42.9%)	0 (0.0%)	0 (0.0%)	3 (13.6%)	
<i>Nodal status</i>						
Node positive	22	4 (57.1%)	5 (50.0%)	4 (36.4%)	9 (40.9%)	0.805
<i>Histological grading</i>						
G 1	4	0 (0.0%)	0 (0.0%)	1 (9.1%)	3 (13.6%)	0.163
G 2	34	3 (42.9%)	8 (64.7%)	6 (54.5%)	17 (77.3%)	
G 3	11	4 (57.1%)	2 (35.3%)	3 (27.4%)	2 (9.1%)	
<i>Genomic grading</i>						
High genomic grade	28	3 (42.9%)	9 (90.0%)	11 (100%)	5 (22.7%)	< 0.001
<i>Estrogen receptor status</i>						
ER + (IHC)	33	3 (42.9%)	2 (20.0%)	7 (63.6%)	21 (95.5%)	< 0.001
ER + (microarray)	31	1 (14.3%)	2 (20.0%)	7 (63.6%)	21 (95.5%)	< 0.001
<i>Her - 2 status</i>						
Her -2+	21	2 (28.6%)	5 (50.0%)	8 (72.7%)	6 (27.3%)	0.072

Tumors were classified by hierarchical clustering according to the intrinsic gene set using 120 marker genes originally described by Sorlie et al.² The different subgroups were compared with clinico-pathological data as well as tumor response to neoadjuvant chemotherapy.

The trial design of the neoadjuvant GEPARTRIO trial¹⁴ was as follows. At first all patients received two cycles of TAC (doxorubicin 50mg/m², cyclophosphamide 500mg/m² and docetaxel 75mg/m² all on day 1, every 3 weeks). Tumor response was determined by palpation during the third week of the second cycle. Patients who demonstrated a tumor response defined as a tumor shrinkage of more than 50% were randomized for four or six further cycles of TAC. In case of no tumor response patients received either four further cycles of TAC or four cycles of NX (vinorelbine 25mg/m² day 1 and 8 plus capecitabine 1000mg/m² orally twice/

day on days 1–14 every 3 weeks) as a non-crossresistant schedule after randomization.

Clinical assessment of tumor response was evaluated by palpation, breast ultrasound and/or mammography and/or MRI. Clinical response was determined at every cycle by palpation and ultrasound. The clinical tumor response after the initial two cycles of TAC was assessed for further randomization. Tissue removed at surgery was investigated by pathologic examination.

A pCR was defined as no microscopic evidence of residual invasive and non-invasive tumor including single tumor cells both in all specimens of the

breast and lymph nodes. Patients who showed a tumor response of at least 50% were classified as partial response (PR) and less than 50% as non-responders (NR). After completion of neoadjuvant therapy patients were monitored for tumor relapse.

Results

Sufficient amounts of RNA for microarray analysis were isolated from two-thirds of 70 biopsies and high-quality data were obtained for $n = 50$ samples (71.4%). The clinical data and response rates of this cohort were described previously⁹ and are iterated in Table 1. Overall we observed a rate of 16% for achieving pCR by TAC chemotherapy, which is in line with the results of the pilot study reported by von Minckwitz et al.¹⁴ (17.9%). Among the clinical parameters only ER-negativity was associated with a higher chance of pCR (pCR rates: ER–12%, ER+4%, $P = 0.013$).⁹ We used 120 Affymetrix probe sets corresponding to the “intrinsic genes” previously described by Sorlie et al.,² which characterize the four different molecular tumor classes. The tumor samples were stratified according to these markers by unsupervised hierarchical clustering. This approach resulted in a stratification of the pretherapeutic samples from the GEPARTRIO trial in the four known molecular tumor subtypes as presented in Table 1 and Supplementary Figure SF1. About 14% of the samples could be assigned to the normal-like, 20% to the basal-like, 22% to erbB2+ and 44% to the luminal subgroup. Menopausal status, tumor stage, nodal status and histopathological grading revealed no statistically significant difference between these subgroups (Table 1). However, high “genomic grading”¹³ was observed for 100% of the erbB2+ and 90% of the basal-like tumors compared to 42.9% in the normal-like and 22.7% in the luminal subgroups ($P < 0.001$). In agreement, we detected high expression of cell cycle associated genes in both basal-like as well as erbB2+ tumor groups but not in normal-like and rarely in luminal breast cancers (Supplementary Figure SF1). Furthermore, the ER status as evaluated by immunohistochemistry (IHC) showed a significant difference between the groups (proportion of ER positive tumors: normal-like: 42.9%, basal-like: 20%, erbB2+: 63.6% and luminal: 95.5%, $P < 0.001$). Comparing these results with ESR1 mRNA expression on the microarray the basal-like, erbB2 and luminal subgroup showed identical expression rates compared to IHC except tumors of the normal-like subgroup, in which only 14.3% of all tumors were ER positive when evaluated by microarray. Interestingly, about two-thirds of all tumors in the erbB2+ subgroup

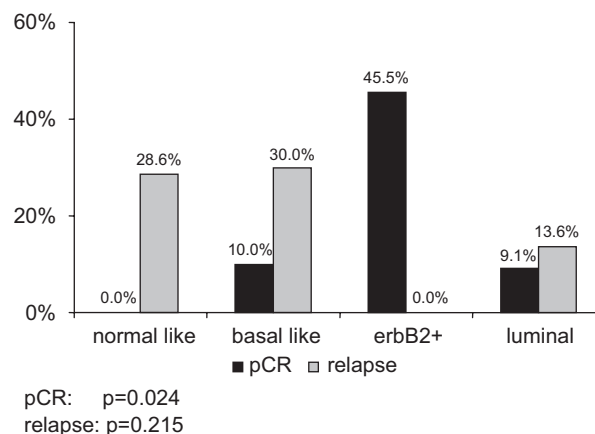


Figure 1 Correlation of molecular tumor subtypes and response to neoadjuvant chemotherapy.

were ER positive both for IHC as well as microarray expression. Her-2 positivity evaluated either by IHC or fluorescence in situ hybridization (FISH) trended to be higher in the erbB2 (72.7%) and the basal-like cluster (50%) compared to the normal-like (28.6%) and luminal subgroup (27.3%, $P = 0.072$).

Figure 1 presents the correlation of pCR to NAC and the molecular subtype of the tumors as well as the observed relapses during followup in the different subgroups. A significant higher portion of patients with a pCR was observed in the erbB2+ subgroup with 45.5% compared to no pCR in the normal-like group and 10% among the basal-like and 9.1% in the luminal subtypes ($P = 0.024$, Fig. 1). Regarding the clinical response there was no statistically significant difference between the subgroups. Furthermore, there was a trend towards a lower number of tumor relapse in the erbB2+ subgroup (erbB2+: no relapse, normal-like: 28.6%, basal-like: 30%, luminal: 13.6%, $P = 0.215$).

Discussion

Our data demonstrate, that the different molecular subtypes of breast cancer described by the intrinsic gene set of Sorlie and colleagues² are characterized by distinct response rates to NAC using a taxane- and anthracycline-containing regimen.

These results are in line with the data of Rouzier et al.⁸ who could demonstrate that tumors in the erbB2+ subgroup show a higher probability of a pCR after NAC (pCR rate Rouzier: 45%, our data: 45.5%). However, we were yet unable to confirm, that the basal-like subgroup is even at a high chance to achieve a pCR (pCR rate Rouzier: 45%, our data 10%), which might be attributed to a higher proportion of ER+ breast cancers (20% vs. 5%) and

a lower proportion of tumors with high histopathological grading (35.3% vs. 91%) in our subgroup. Our data and the data of Rouzier et al. demonstrate that the molecular tumor classification according to the intrinsic gene set is highly reproducible and has power to predict response to NAC. Even though the erbB2+ subgroup has the highest chance to achieve a pCR after NAC, the Her-2 status itself alone is not at all predictive in our cohort (pCR Her-2⁺ vs. Her-2⁻: 5.1% vs. 5.1%, $P = 1.0$). This was also observed by Rouzier et al. in a multivariate analysis (odds ratio Her-2+: 1.77 (95% CI: 0.42–7.5), $P = 0.43$),⁸ suggesting that other molecular markers in this subgroup are of relevance. Data regarding the predictive value of Her-2 expression in NAC are inconsistent. The clinical results of the GEPAR-TRIO pilot study did not show a correlation between Her-2 status (assessed by FISH analysis) and tumor response.¹⁴ Learn et al.¹⁵ could demonstrate that women who had HER-2 negative tumors appeared to have a lower response rate with neoadjuvant doxorubicin/cyclophosphamide chemotherapy alone compared with women who had HER-2-positive tumors (51% vs. 75%; $P = 0.06$), but response rates were matched when docetaxel was added (81% vs. 78%; $P = 0.99$). Interestingly ER, PR, p53, and Ki-67 results were not associated significantly with response rates. However, in our cohort we could reveal that Ki-67 is predictive to achieve pCR (Pearson χ^2 : 5.357, $P = 0.021$, data not shown).

Konecny et al. could show improved response rates in patients with advanced, Her-2 positive breast cancer receiving a combination of epirubicine and paclitaxel.¹⁶ In the adjuvant setting Roche et al. could demonstrate in a retrospective analysis of PACS01 trial an improved DFS and OS in patients with Her-2 overexpression or amplification by the treatment with the combination of 5-fluorouracil, epirubicine and cyclophosphamide (FEC) followed by docetaxel, compared to patients receiving FEC alone.¹⁷

Although ER-negativity is good marker for tumor response to NAC (pCR ER–: 12% vs. ER+: 4%, $P = 0.013$) a substantial proportion of ER+ breast cancers is observable in the erbB2 cluster (63.6%). This might suggest that ER+ tumors have a sufficient propability to achieve a pCR if they can be attributed to the erbB2+ subtype by molecular classification. Our data demonstrate that molecular classification is helpful in order to establish prognosis of breast cancer patients and also to predict the success of specific therapeutic approaches. Since these result further support the intrinsic differences between the molecular breast cancer subtypes, and emphasize the importance of the Sorlie classification it is eligible to confirm these results in a larger cohort.

Acknowledgments

We thank Katherina Kourtis for expert technical assistance. This work was supported by grants from the Deutsche Krebshilfe, Bonn, the Margarete Bonifer-Stiftung, Bad Soden, the BANSS-Stiftung, Biedenkopf, and the Dr. Robert Pflieger-Stiftung, Bamberg.

Appendix A. Supplementary materials

Supplementary data associated with this article can be found in the online version at [doi:10.1016/j.breast.2007.02.006](https://doi.org/10.1016/j.breast.2007.02.006).

References

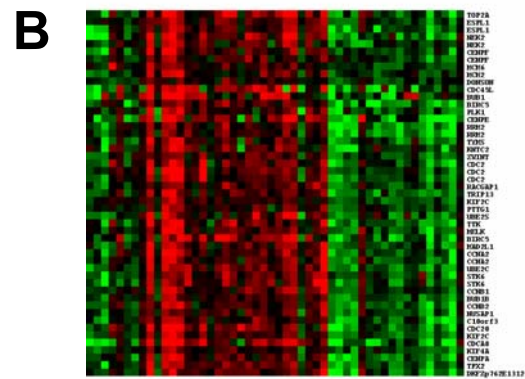
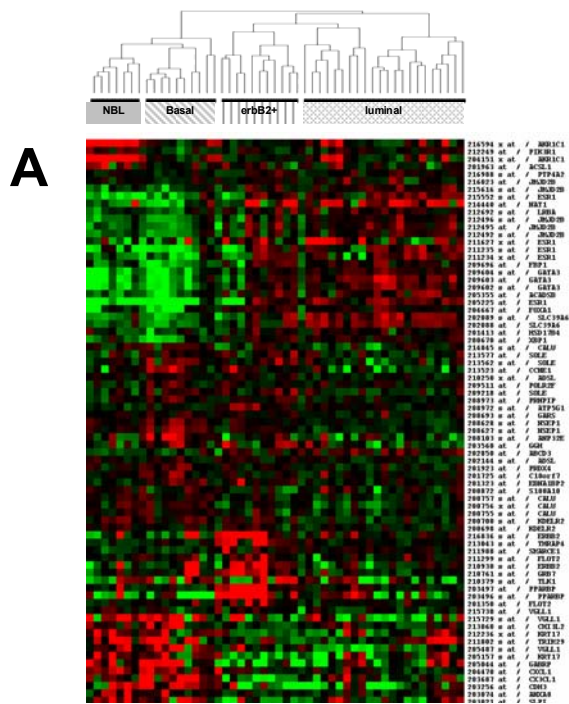
1. Kaufmann M, Hortobagyi GN, Goldhirsch A, Scholl S, Makris A, Valagussa P, et al. Recommendations from an international expert panel on the use of neoadjuvant (primary) systemic treatment of operable breast cancer: an update. *J Clin Oncol* 2006;**24**(12):1940–9.
2. Sorlie T, Perou CM, Tibshirani R, Aas T, Geisler S, Johnsen H, et al. Gene expression patterns of breast carcinomas distinguish tumor subclasses with clinical implications. *Proc Natl Acad Sci USA* 2001;**98**:10869–74.
3. van de Vijver MJ, He YD, van't Veer LJ, Dai H, Hart AA, Voskuil DW, et al. A gene-expression signature as a predictor of survival in breast cancer. *N Engl J Med* 2002;**347**:1999–2009.
4. Ahr A, Karn T, Solbach C, Seiter T, Strebhardt K, Holtrich U, et al. Identification of high risk breast-cancer patients by gene expression profiling. *Lancet* 2002;**359**:131–2.
5. Wang Y, Klijn JG, Zhang Y, Sieuwerts AM, Look MP, Yang F, et al. Gene-expression profiles to predict distant metastasis of lymph-node-negative primary breast cancer. *Lancet* 2005;**365**(9460):671–9.
6. Perou CM, Jeffrey SS, van de Rijn M, Rees CA, Eisen MB, Ross DT, et al. Distinctive gene expression patterns in human mammary epithelial cells and breast cancers. *Proc Natl Acad Sci USA* 1999;**96**:9212–7.
7. Sorlie T, Tibshirani R, Parker J, Hastie T, Marron JS, Nobel A, et al. Repeated observation of breast tumor subtypes in independent gene expression data sets. *Proc Natl Acad Sci USA* 2003;**100**(14):8418–23.
8. Rouzier R, Perou CM, Symmans WF, Ibrahim N, Cristofanilli M, Anderson K, et al. Breast cancer molecular subtypes respond differently to preoperative chemotherapy. *Clin Cancer Res* 2005;**11**:5678–85.
9. Rody A, Karn T, Gatje R, Ahr A, Solbach C, Kourtis K, et al. Gene expression profiling of breast cancer patients treated with docetaxel, doxorubicin, and cyclophosphamide within the GEPARTRIO trial: HER-2, but not topoisomerase II alpha and microtubule-associated protein tau, is highly predictive of tumor response. *Breast* 2007;**16**(1):86–93.
10. Modlich O, Prisack HB, Munnes M, Audretsch W, Bojar H. Predictors of primary breast cancers responsiveness to preoperative epirubicin/cyclophosphamide-based chemotherapy: translation of microarray data into clinically useful predictive signatures. *J Transl Med* 2005;**3**:32.

11. Rody A, Holtrich U, Gatje R, Gehrman M, Engels K, von Minckwitz G, et al. Poor outcome in estrogen receptor-positive breast cancers predicted by loss of Plexin B1. *Clin Cancer Res* 2007;**13**(4):1210–8.
12. Eisen MB, Spellman PT, Brown PO, Botstein D. Cluster analysis and display of genome-wide expression patterns. *Proc Natl Acad Sci USA* 1998;**95**(25):14863–8.
13. Sotiriou C, Wirapati P, Loi S, Harris A, Fox S, Smeds J, et al. Gene expression profiling in breast cancer: understanding the molecular basis of histologic grade to improve prognosis. *J Natl Cancer Inst* 2006;**98**:262–72.
14. von Minckwitz G, Blohmer JU, Raab G, Lohr A, Gerber B, Heinrich G, et al. In vivo chemosensitivity-adapted preoperative chemotherapy in patients with early-stage breast cancer: the GEPARTRIO pilot study. *Ann Oncol* 2005;**16**:56–63.
15. Learn PA, Yeh IT, McNutt M, Chisholm GB, Pollock BH, Rousseau Jr DL, et al. HER-2/neu expression as a predictor of response to neoadjuvant docetaxel in patients with operable breast carcinoma. *Cancer* 2005;**103**: 2252–60.
16. Konecny GE, Thomssen C, Luck HJ, Untch M, Wang HJ, Kuhn W, et al. Her-2/neu gene amplification and response to paclitaxel in patients with metastatic breast cancer. *J Natl Cancer Inst* 2004;**96**:1141–51.
17. Roche HH, Penault-Llorca FM, Sagan C, Lacroix-Triki M, Denoux Y, Verrielle V, et al. Prognostic and predictive value of HER2, PR, ER, and KI67 in the PACS01 trial comparing epirubicin-based chemotherapy to sequential epirubicin followed by docetaxel. *J Clin Oncol* 2005;**23**(16S) (abstr. 605).

Available online at www.sciencedirect.com



Supplementary Figure SF1:



Supplementary Table 1:

Sorlie subtype	Affymetrix Probe Set	Gene Symbol	RefSeq	Description
luminal	222033_s_at	ZYX	NM_002019	U01134 soluble vascular endothelial cell growth factor receptor (sflt) fms-related tyrosine kinase 1 (vascular endothelial growth factor/vascular permeability factor receptor) fms-related tyrosine kinase 1 (vascular endothelial growth factor/vascular permeability factor receptor)
luminal	219872_at	DKFZp434L142	NM_016613	zps59c06.s1 AD021 protein
luminal	219197_s_at	SCUBE2	NM_020974	wv11f12.x1 CEGP1 protein
luminal	218807_at	VAV3	NM_006113	HUMGS0005283 vav 3 oncogene EST
luminal	218806_s_at	VAV3	NM_006113	zh47f03.r1 VAV-3 protein (VAV-3) alternatively spliced vav 3 oncogene EST
luminal	218259_at	MKL2	NM_014048	yc83f03.r1 KIAA1243 protein EST
luminal	216988_s_at	PTP4A2	NM_003479	protein-tyrosine phosphatase (HU-PP-1) sequence (clone hh18) protein tyrosine phosphatase (ptp-IV1r) gene 5 end of c protein tyrosine phosphatase type IVA member 2 protein tyrosine phosphatase type IVA, member 2
luminal	216023_at	JMJD2B	NM_015015	: FLJ22387 fis clone HRC07655
luminal	215616_s_at	JMJD2B	NM_015015	KIAA0876 protein for KIAA0876 protein KIAA0876 protein KIAA0876 protein
luminal	215552_s_at	ESR1	NM_000125	DNA sequence from clone RP1-6315 on chromosome 6q25.1-26. Contains the 3 part of a novel gene and an exon of the ESR1 gene for estrogen receptor 1 (NR3A1 estradiol receptor) ESTs STSs and GSSs
luminal	215551_at	ESR1	NM_000125	DNA sequence from clone RP1-6315 on chromosome 6q25.1-26. Contains the 3 part of a novel gene and an exon of the ESR1 gene for estrogen receptor 1 (NR3A1 estradiol receptor) ESTs STSs and GSSs
luminal	214552_s_at	RABEP1	NM_004703	rabaptin-4 rabaptin-4 d rabaptin-5 rabaptin-4
luminal	214440_at	NAT1	NM_000662	liver arylamine N-acetyltransferase (EC 2.3.1.5) gene N-acetyltransferase 1 (arylamine N-acetyltransferase)
luminal	214109_at	LRBA	NM_006726	beige-like protein (BGL) cell division cycle 4-like similar to yeast YCR032w, GenBank Accession Number X59720, Mus musculus BG, GenBank Accession Number U52461 and C. elegans F10F2.1, GenBank Accession Number Z35598; previously identified as CDC4L beige-1
luminal	212770_at	TLE3	NM_005078	DKFZp566A114_r1 KIAA1547 protein EST
luminal	212769_at	TLE3	NM_005078	transducin-like enhancer protein (TLE3) transducin-like enhancer of split 3 homolog of Drosophila transducin-like enhancer of split 3 homolog of Drosophila E(sp1) KIAA1547 protein
luminal	212692_s_at	LRBA	NM_006726	beige-like protein (BGL) cell division cycle 4-like similar to yeast YCR032w, GenBank Accession Number X59720, Mus musculus BG, GenBank Accession Number U52461 and C. elegans F10F2.1, GenBank Accession Number Z35598; previously identified as CDC4L beige-1
luminal	212496_s_at	JMJD2B	NM_015015	ng44h07.s1 KIAA0876 protein EST
luminal	212495_at	JMJD2B	NM_015015	ng44h07.s1 KIAA0876 protein EST
luminal	212492_s_at	JMJD2B	NM_015015	za24c10.r1 KIAA0876 protein
luminal	211627_x_at	ESR1	NM_000125	estrogen receptor-related protein (variant ER from breast cancer) d
luminal	211235_s_at	ESR1	NM_000125	HSERR oestrogen receptor estrogen receptor alpha ds alternatively splice estrogen receptor 1 estrogen receptor; receptor; steroid hormone receptor oestrogen receptor
luminal	211234_x_at	ESR1	NM_000125	HSERR oestrogen receptor estrogen receptor alpha ds alternatively splice estrogen receptor 1 estrogen receptor; receptor; steroid hormone receptor oestrogen receptor
luminal	210287_s_at	FLT1	NM_002019	U01134 soluble vascular endothelial cell growth factor receptor (sflt) fms-related tyrosine kinase 1 (vascular endothelial growth factor/vascular permeability factor receptor) fms-related tyrosine kinase 1 (vascular endothelial growth factor/vascular permeability factor receptor)
luminal	209696_at	FBP1	NM_000507	fructose-1,6-bisphosphatase (FBP1) gene for fructose-1,6-bisphosphatase human liver fructose-1,6-bisphosphatase deficiency; gene structure; mutations fructose-bisphosphatase 1
luminal	209604_s_at	GATA3	NM_001002295	hGATA3 trans-acting T-cell specific transcription factor GATA-binding protein 3 clone MGC:23 GATA-binding protein 3 GATA binding protein 3
luminal	209603_at	GATA3	NM_001002295	hGATA3 trans-acting T-cell specific transcription factor GATA-binding protein 3 GATA binding protein 3
luminal	209602_s_at	GATA3	NM_001002295	hGATA3 trans-acting T-cell specific transcription factor GATA-binding protein 3 GATA binding protein 3
luminal	208617_s_at	PTP4A2	NM_003479	protein-tyrosine phosphatase (HU-PP-1) sequence protein tyrosine phosphatase type IVA member 2 protein tyrosine phosphatase type IVA, member 2
luminal	208616_s_at	PTP4A2	NM_003479	HSU14603 protein-tyrosine phosphatase (HU-PP-1) sequence protein tyrosine phosphatase PTPCAA2 (HPTPCAA2) d protein tyrosine phosphatase type IVA member 2 similar to rat tyrosine phosphatase encoded by GenBank Accession Number L27843 protein-tyrosine phosphatase
luminal	208615_s_at	PTP4A2	NM_003479	protein-tyrosine phosphatase (HU-PP-1) sequence protein tyrosine phosphatase type IVA member 2 protein tyrosine phosphatase type IVA, member 2
luminal	206472_s_at	TLE3	NM_005078	transducin-like enhancer of split 3 homolog of Drosophila E(sp1) transducin-like enhancer of split 3 (E(sp1) homolog
luminal	205355_at	ACAD9B	NM_001609	acyl-CoA dehydrogenase acyl-Coenzyme A dehydrogenase short/branched chain (ACAD9B) nuclear gene encoding mitochondrial prote acyl-Coenzyme A dehydrogenase short/branched chain acyl-Coenzyme A dehydrogenase, short/branched chain
luminal	205225_at	ESR1	NM_000125	HSERR oestrogen receptor estrogen receptor 1 estrogen receptor; receptor; steroid hormone receptor oestrogen receptor
luminal	204667_at	FOXA1	NM_004496	hepatocyte nuclear factor 3 alpha hepatocyte nuclear factor 3, alpha
luminal	204406_at	FLT1	NM_002019	U01134 soluble vascular endothelial cell growth factor receptor (sflt) fms-related tyrosine kinase 1 (vascular endothelial growth factor/vascular permeability factor receptor) fms-related tyrosine kinase 1 (vascular endothelial growth factor/vascular permeability factor receptor)
luminal	203223_at	RABEP1	NM_004703	unknown protein of uterine endometrium rabaptin-5 antigen; uterine endometrium protein
luminal	202089_s_at	SLC39A6	NM_012319	HSU41060 breast cancer estrogen regulated LIV-1 protein (LIV-1) LIV-1 protein estrogen regulated estrogen regulated mRNA; breast cancer LIV-1 protein LIV-1 protein, estrogen regulated
luminal	202088_at	SLC39A6	NM_012319	HSU41060 breast cancer estrogen regulated LIV-1 protein (LIV-1) LIV-1 protein estrogen regulated estrogen regulated mRNA; breast cancer LIV-1 protein LIV-1 protein, estrogen regulated
luminal	201413_at	HSD17B4	NM_000414	17-beta-hydroxysteroid dehydrogenase hydroxysteroid (17-beta) dehydrogenase 4 17-beta-hydroxysteroid dehydrogenase hydroxysteroid (17-beta) dehydrogenase 4
luminal	200670_at	XBP1	NM_005080	DNA sequence from clone 292E10 on chromosome 22q11-12. Contains the XBPT1 gene X-box binding protein 1 (TREB5) ESTs STSs GSSs and a putative CpG island X-box binding protein 1
luminal	221803_s_at	NRBF2	NM_030759	am18h01.s1 Similar to nuclear receptor binding factor nuclear receptor binding factor-2
luminal	221505_at	ANP32E	NM_030920	at14a02.x1 : FLJ21971 fis clone HEP05790 EST hypothetical protein MGC5350
luminal	218728_s_at	HSPC163	NM_014184	zk67h12.s1 HSPC163 protein EST
luminal	218051_s_at	FLJ12442	NM_022908	hypothetical protein FLJ12442
luminal	217733_s_at	TMSB10	NM_021103	thymosin beta-10 gene 3end thymosin beta 10 thymosin beta-10 thymosin, beta 10
luminal	214845_s_at	CALU	NM_001219	crocalbin-like protein ds
luminal	213577_at	SQLE	NM_003129	squalene epoxidase squalene epoxidase squalene epoxidase squalene monoxygenase
luminal	213562_s_at	SQLE	NM_003129	squalene epoxidase squalene epoxidase squalene epoxidase squalene monoxygenase
luminal	213523_at	CCNE1	NM_001238	cyclin cyclin E1
luminal	210250_x_at	ADSL	NM_000026	adenylosuccinate lyase (ADSL) alternatively spliced adenylosuccinate lyase (ADSL) alternatively spliced adenylosuccinate lyase alternatively spliced; adenylosuccinate adenylosuccinate lyase
luminal	209511_at	POLR2F	NM_021974	zv98d05.r1 polymerase (RNA) II (DNA directed) polypeptide F clone MGC:26 polymerase (RNA) II (DNA directed) polypeptide F EST
luminal	209218_at	SQLE	NM_003129	squalene epoxidase squalene epoxidase (ERG1) d squalene epoxidase squalene epoxidase squalene monoxygenase
luminal	208973_at	PRNP	XM_290941	clone 23856 unknown Unknown (protein for MGC-2883) Homo sapiens clone 23856 unknown mRNA partial cds prion protein interacting protein
luminal	208972_s_at	ATP5G1	NM_001002027	genemitochondrial ATP synthase c subunit (P1 form) ATP synthase H+ transporting mitochondrial F0 complex subunit c (subunit 9) isoform 1
luminal	208693_s_at	GARS	NM_002047	glycyl-tRNA synthetase T-cell for glycyl tRNA synthetase d glycyl-tRNA synthetase GlyRS glycyl-tRNA synthetase
luminal	208628_s_at	NSEP1	NM_004559	Y box binding protein-1 (YB-1) nuclease sensitive element binding protein 1 Y box binding protein Y box binding protein-1 nuclease sensitive element binding protein 1
luminal	208627_s_at	NSEP1	NM_004559	Y box binding protein-1 (YB-1) nuclease sensitive element binding protein 1 Y box binding protein Y box binding protein-1 nuclease sensitive element binding protein 1
luminal	208103_s_at	ANP32E	NM_030920	o139a08.s1 : FLJ21971 fis clone HEP05790
luminal	203560_at	GGH	NM_003878	gamma-glutamyl hydrolase (GGH) gamma-glutamyl hydrolase (conjugase felypolygamma-glutamyl hydrolase) precursor gamma-glutamyl hydrolase (conjugase felypolygamma-glutamyl hydrolase) gamma-glutamyl hydrolase (conjugase, felypolygamma-glutamyl hydrolase) pre
luminal	202850_at	ABCD3	NM_002858	PXMP1 gene exon 1 (and joined CDS) ATP-binding cassette sub-family (ALD) member 3 PXMP1 gene 70kD peroxisomal integral membrane protein ATP-binding cassette, sub-family D (ALD), member 3
luminal	202144_s_at	ADSL	NM_000026	adenylosuccinate lyase (ADSL) alternatively spliced adenylosuccinate lyase alternatively spliced; adenylosuccinate adenylosuccinate lyase
luminal	201923_at	PRDX4	NM_006406	antioxidant enzyme AOE3-2 thioredoxin peroxidase (antioxidant enzyme) peroxiredoxin 4

luminal	201725_at	C10orf7	NM_006023	protein D123 D123 gene product
luminal	201323_at	EBNA1BP2	NM_006824	nucleolar protein p40 nucleolar protein p40 homolog of yeast EBNA1-binding protein nucleolar protein p40 cell proliferation-associated protein nucleolar protein p40 EBNA1 binding protein 2
luminal	200872_at	S100A10	NM_002966	q71b11.1 x1 S100 calcium-binding protein A10 (annexin II ligand calpactin I light polypeptide (p11)) S100 calcium binding protein A10 (annexin II ligand,
luminal	200757_s_at	CALU	NM_001219	calumenin (Calu) calumenin precursor calumenin member of one subset of EF-hand superfamily that includes reticulocalbin, Erc-55, and Cab-45 calumenin precursor
luminal	200756_x_at	CALU	NM_001219	ak42e07.s1 calumenin d ESTs Moderately similar to OPSB HUMAN BLUE-SENSITIVE OPSIN [H.sapiens]
luminal	200755_s_at	CALU	NM_001219	ak42e07.s1 calumenin ESTs Moderately similar to OPSB HUMAN BLUE-SENSITIVE OPSIN [H.sapiens]
luminal	200700_s_at	KDELR2	NM_006854	ELP-1 sequence KDEL (Lys-Asp-Glu-Leu) endoplasmic reticulum protein retention receptor 2
luminal	200698_at	KDELR2	NM_006854	ELP-1 sequence KDEL (Lys-Asp-Glu-Leu) endoplasmic reticulum protein retention receptor 2
erbB2+	218464_s_at	FLJ10700	NM_018182	zd84c11.r1 hypothetical protein FLJ10700
erbB2+	216836_s_at	ERBB2	NM_001005862	tyrosine kinase-type receptor (HER2) v-erb-b2 avian erythroblastic leukemia viral oncogene homolog 2 (neuroglioblastoma derived oncogene homolog) v-erb-b2 avian erythroblastic leukemia viral oncogene homolog 2 (neuro/glioblastoma derived oncogene homolog)
erbB2+	215337_at	TRAP100	NM_014815	KIAA0130 gene FLJ12446 fis clone NT2RM1000260 highly similar to thyroid hormone receptor-associated protein complex component TRAP100 mRNA KIAA0130 gene product KIAA0130 The KIAA0130 gene is related to mouse genetic suppressor element (911GSE), KIAA0130 ge
erbB2+	213043_s_at	THRAP4	NM_014815	KIAA0130 gene KIAA0130 gene product KIAA0130 The KIAA0130 gene is related to mouse genetic suppressor element (911GSE), KIAA0130 gene product
erbB2+	211989_at	SMARCE1	NM_003079	BAF57 (BAF57) gene SWI/SNF related matrix associated actin dependent regulator of chromatin subfamily e member 1 SWI/SNF related matrix associated actin dependent regulator of chromatin subfamily e member 1 HMG-domain containing protein which is the 57 kd
erbB2+	211988_at	SMARCE1	NM_003079	BAF57 (BAF57) gene SWI/SNF related matrix associated actin dependent regulator of chromatin subfamily e member 1 SWI/SNF related matrix associated actin dependent regulator of chromatin subfamily e member 1 HMG-domain containing protein which is the 57 kd
erbB2+	211299_s_at	FLOT2	NM_004475	surface antigen Similar to flotillin 2 clone MGC:50 flotillin 2 surface antigen
erbB2+	211077_s_at	TLK1	NM_012290	protein-sennethreonine kinase gene
erbB2+	210930_s_at	ERBB2	NM_001005862	tyrosine kinase-type receptor (HER2) v-erb-b2 avian erythroblastic leukemia viral oncogene homolog 2 (neuroglioblastoma derived oncogene homolog) v-erb-b2 avian erythroblastic leukemia viral oncogene homolog 2 (neuro/glioblastoma derived oncogene homolog)
erbB2+	210761_s_at	GRB7	NM_005310	HUMGRB7 squamous cell carcinoma of esophagus GRB-7 SH2 domain protein growth factor receptor-bound protein 7 GRB-7 SH2 domain protein; growth factor receptor-bound protein 7 GRB-7 SH2 domain protein
erbB2+	210379_s_at	TLK1	NM_012290	KIAA0137 gene tousled-like kinase 1 (TLK1) d tousled-like kinase 1 KIAA0137 protein Start codon is not identified. ha02915 cDNA clone for KIAA0137 has a 1-bp insertion between 359-360, a 262-bp insertion between 363-364, and a 69-bp insertion between 436-
erbB2+	208398_s_at	TBPL1	NM_004865	DNA sequence from clone 73H22 on chromosome 6q23 TBP-like 1 HTG; CpG island dJ73H22.1 (TBP-like protein)
erbB2+	203497_at	PPARBP	NM_004774	RB18A protein thyroid hormone receptor interactor 2 PPAR binding protein p53 regulatory protein; RB18A protein RB18A protein
erbB2+	203496_s_at	PPARBP	NM_004774	RB18A protein thyroid hormone receptor-associated protein complex component TRAP220 d PPAR binding protein p53 regulatory protein; RB18A protein RB18A protein
erbB2+	202606_s_at	TLK1	NM_012290	KIAA0137 gene tousled-like kinase 1 KIAA0137 protein Start codon is not identified. ha02915 cDNA clone for KIAA0137 has a 1-bp insertion between 359-360, a 262-bp insertion between 363-364, and a 69-bp insertion between 436-437 of the sequence of KIAA0137
basal-like	201350_at	FLOT2	NM_004475	surface antigen flotillin 2 surface antigen
basal-like	823_at	CX3CL1	NM_002996	small inducible cytokine subfamily D (Cys-X3-Cys), member 1 (fractalkine, neurotactin)
basal-like	220617_s_at	ZNF532	NM_018181	z148e07.r1 hypothetical protein FLJ10697 EST
basal-like	215730_at	VGLL1	NM_016267	dJ196E23.1.1 (novel protein) (isoform 1) TONDU HIV TAT specific factor 1
basal-like	215729_s_at	VGLL1	NM_016267	dJ196E23.1.1 (novel protein) (isoform 1) TONDU HIV TAT specific factor 1
basal-like	213060_s_at	CHI3L2	NM_004000	chitinase (HUMTCHT)exon 1b form chitinase (HUMTCHT) exon 1b form d chitinase 3-like 2 submtter can find no appropriate Kozak initiator methionine, despite the open reading frame continuing upstream, and is certain that there are no other exons 5' as det
basal-like	212236_x_at	KRT17	NM_000422	genecytokeratin 17 gene for cytokeratin keratin 17 cytokeratin 17
basal-like	211002_s_at	TRIM29	NM_012101	HUMDK ataxia-telangiectasia group D-associated protein tripartite motif protein TRIM29 beta d ataxia-telangiectasia group D-associated protein ataxia-telangiectasia group D-associated protein tripartite motif-containing 29
basal-like	211001_at	TRIM29	NM_012101	HUMDK ataxia-telangiectasia group D-associated protein tripartite motif protein TRIM29 beta d ataxia-telangiectasia group D-associated protein ataxia-telangiectasia group D-associated protein tripartite motif-containing 29
basal-like	210605_s_at	MFGE8	NM_005928	breast epithelial antigen BA46 Similar to milk fat globule-EGF factor 8 protein clone MGC:13 milk fat globule-EGF factor 8 protein breast epithelial antigen BA46
basal-like	205487_s_at	VGLL1	NM_016267	dJ196E23.1.1 (novel protein) (isoform 1) TONDU HIV TAT specific factor 1
basal-like	205157_s_at	KRT17	NM_000422	genecytokeratin 17 keratin 17 cytokeratin 17
basal-like	205044_at	GABRP	NM_014211	GABA-A receptor pi subunit gamma-aminobutyric acid (GABA) A receptor pi gamma-aminobutyric acid (GABA) A receptor, pi
basal-like	204470_at	CXCL1	NM_001511	HSMGSA9 genemelanoma growth stimulatory activity (MGS) GRO1 oncogene (melanoma growth stimulating activity alpha) GRO1 oncogene (melanoma growth stimulating activity)
basal-like	204087_s_at	SLC5A6	NM_021095	DKFZp434F152 (from clone DKFZp434F152) solute carrier family 5 (sodium-dependent vitamin transporter) member 6 Homo sapiens mRNA; cDNA DKFZp434F152 (from clone DKFZp434F152) solute carrier family 5 (sodium-dependent vitamin transporter)
basal-like	203706_s_at	FZD7	NM_003507	frizzled-7 frizzled (Drosophila) homolog 7 frizzled-7 frizzled homolog 7 (Drosophila)
basal-like	203705_s_at	FZD7	NM_003507	frizzled-7 frizzled (Drosophila) homolog 7 frizzled-7 frizzled homolog 7 (Drosophila)
basal-like	203687_at	CX3CL1	NM_002996	HSU84487 CX3C chemokine precursor alternatively spliced small inducible cytokine subfamily(Cys-X3-Cys) member 1 (fractalkine neurotactin) small inducible cytokine subfamily D (Cys-X3-Cys), member
basal-like	203256_at	CDH3	NM_001793	cadherin 3 type 1 P-cadherin (placental)
basal-like	203188_at	B3GNT6	NM_006876	i-beta-1 3-N-acetylglucosaminyltransferase i-beta-1 3-N-acetylglucosaminyltransferase glycosyltransferase; poly-N-acetyllactosamine extension enzyme i-antigen; iGnT i-beta-1,3-N-acetylglucosaminyltransferase UDP-GlcNAc:betaGal beta-1,3-N-acetylglucosaminyl
basal-like	203074_at	ANXA8	NM_001630	vascular anticoagulant-beta (VAC-beta) annexin VIII annexin A8 annexin; calcium binding protein; phospholipase a2 inhibitor; phospholipid-binding protein; vascular anticoagulant vascular anticoagulant-beta (AA 1 - 327) annexin VIII
basal-like	203021_at	SLPI	NM_003064	antileukoprotease (ALP) from cervix uterus secretory leukocyte protease inhibitor (antileukoprotease) antileukoprotease; elastase inhibitor; protease; signal peptide precursor ALP secretory leukocyte protease inhibitor (antileukoprotease)
basal-like	202504_at	TRIM29	NM_012101	HUMDK ataxia-telangiectasia group D-associated protein ataxia-telangiectasia group D-associated protein ataxia-telangiectasia group D-associated protein tripartite motif-containing 29
basal-like	202013_s_at	EXT2	NM_000401	multiple exostoses 2 (EXT2) gene exostoses (multiple) 2 exostoses (multiple) 2
basal-like	202012_s_at	EXT2	NM_000401	multiple exostoses type II protein EXT2.I exostoses (multiple) 2 isoform of EXT2 exostoses (multiple) 2
basal-like	201820_at	KRT5	NM_000424	HUMKER2A keratin type II (58 kd) keratin 5 (epidermolysis bullosa simplex Dowling-Meara/Kobner/Weber-Cockayne types) keratin 5 (epidermolysis bullosa simplex Dowling-Meara/Kobner/Weber-Cockayne types)
NB-like	217626_at	AKR1C1	NM_001353	ESTs Highly similar to I53872 dihydrodiol dehydrogenase
NB-like	216594_x_at	AKR1C1	NM_001353	hepatic dihydrodiol dehydrogenase gene c 20-alpha (3-alpha)-hydroxysteroid deh hepatic dihydrodiol dehydrogenase
NB-like	212249_at	PIK3R1	NM_181504	P13-kinase associated p85 sequence phosphoinositide-3-kinase regulatory subunit polypeptide 1 (p85 alpha) P13-kinase; tyrosine kinase receptor
NB-like	212240_s_at	PIK3R1	NM_181504	HUMP13KIN P13-kinase associated p85 sequence phosphoinositide-3-kinase regulatory subunit polypeptide 1 (p85 alpha) P13-kinase; tyrosine kinase receptor
NB-like	210879_s_at	RAB11FIP5	NM_015470	KIAA0857 protein Rab11 interacting protein Rip11a d KIAA0857 protein KIAA0857 protein
NB-like	204151_x_at	AKR1C1	NM_001353	hepatic dihydrodiol dehydrogenase gene aldo-keto reductase family 1 member C1 (dihydrodiol dehydrogenase 1 20-alpha (3-alpha)-hydroxysteroid dehydrogenase) hepatic dihydrodiol dehydrogenase aldo-keto reductase family 1, member C1 (dihydrodiol)
NB-like	202645_s_at	MEN1	NM_000244	HSU93237 menin (MEN1) gene multiple endocrine neoplasia 1
NB-like	201963_at	ACSL1	NM_001995	long-chain acyl-CoA synthetase fatty-acid-Coenzyme A ligase long-chain 2 fatty-acid-Coenzyme A ligase, long-chain 2